Supplemental Information

Secondary Analyses: Multivariate Autoregressive (MAR) Modeling

MAR Methods. While partial cross correlation (PCC) examines simultaneous relationships, it does not capture dynamic (time lagged) relationships among regions of interest (ROIs). Instead, MAR modeling is a potential means to address the question "Is the BOLD signal in one ROI associated with the past BOLD signal in other regions?"(1). MAR links ROIs via a regression model to explicitly characterize whether the BOLD signal at one ROI is associated with the past BOLD signal at other ROIs—i.e., "How do the BOLD fluctuations at one ROI at time point t influence subsequent fluctuations at another ROI at future time points t+1, t+2…?" (2;3). When a MAR connectivity coefficient significantly differs from zero, this suggests the presence of Granger-Causality—i.e., resting state functional connectivity (RSFC) BOLD signal in one ROI predicted that in another—although work in the interpretation of MAR is rapidly evolving (4).

MAR models were fit to our three a priori ROIs and iterative right superior temporal gyrus (STG) ROI from our primary analyses (see "Results"). The BOLD signal for the four ROIs is $V(t)=[V_1(t), V_2(t), V_3(t), V_4(t)]$. The MAR model relates BOLD signal at time t to previous time points via the connectivity coefficient matrices Φ_1 through Φ_p. The MAR model is $V(t)=\Phi_1 V(t-1) +\ldots+ \Phi_p V(t-p) +E(t)$, where E(t) is assumed to be a multivariate Gaussian white noise. The lag order p for MAR is selected via the Bayesian information criterion (BIC), as the sum of 1) the log-likelihood (giving the least squares fit) and 2) the complexity penalty, which increases with p. The best lag gives a good fit with a reasonable level of complexity, which was p = 4 for our analyses. The coefficient matrix Φ_k indicates how BOLD signal at time

point t-k affects the BOLD signal at time t. The element $\Phi_{k,ij}$ is the regression *connectivity coefficient* that relates the BOLD signal at ROI_i at time t as a function of the BOLD signal at ROI_j at the previous time point t_{-k}. Non-zero diagonal elements of the matrices indicate the presence of Granger-causality. The connectivity coefficient matrices were denoted Φ for controls and Ψ for the bipolar disorder (BD) group. The connectivity coefficient parameters in the MAR model were estimated using the conditional least squares simultaneously using all participants. Rather than a two-stage approach (step 1 = compute subject-specific estimates separately; step 2 = use some summarized measures of the individual estimates), we performed a single-stage approach because it gives higher power to detect between-group differences by using more data to estimate error variance (and hence has higher degrees of freedom). To test for differences in the connectivity parameters, $\Delta_{k,ij} = \Phi_{k,ij} - \Psi_{k,ij}$ (difference at time lag k in connectivity for $ROIs_{ij}$ – between healthy controls and BD children), we used asymptotic Gaussian theory for conditional least squares estimators.

MAR Results. We found three significant within-groups results ($p < 0.001$) using MAR models among our three a priori and iterative STG ROIs. First, among BD youths, spontaneous BOLD signal in the STG depended on activity at the dorsolateral prefrontal cortex (DLPFC) and amygdala at t-1, t-2, and t-3. In controls, spontaneous BOLD signal in the STG was not predicted by prior spontaneous fluctuations in any ROIs tested. Second, among BD youths, spontaneous BOLD fluctuations in the amygdala depended on activity in the accumbens at t-1 and t-2. In controls, this relationship was two-way, with amygdala activity depending on accumbens at t-1, t-2, and t-4, and accumbens activity depending on amygdala at t-1 and t-2. Third, among BD participants, spontaneous activity in the accumbens and the DLPFC mutually

influenced each another, whereas in healthy controls (HC), activity in the accumbens and DLPFC were not interdependent (Figure S1).

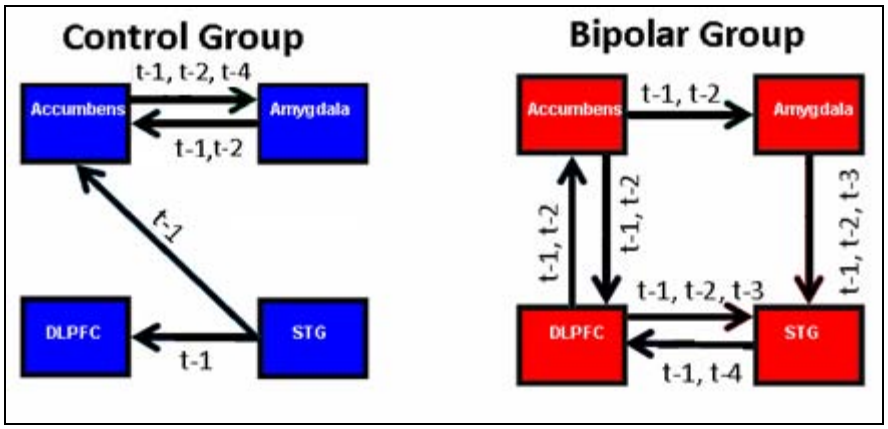

Figure S1. Multivariate autoregressive (MAR) model of resting state functional connectivity (RSFC) indicates altered fronto-temporal functional connectivity in pediatric bipolar disorder (Right) vs. typically-developing healthy controls (Left). Method: Arrows are oriented to point from the ROI whose t-n lagged spontaneous RSFC activity influences the other ROI. Note the following significant differences:

(a) In the pediatric BD group, the RSFC in the STG appears to depend on the spontaneous activity in the dorsolateral prefrontal cortex (DLPFC) and amygdala at t-1, t-2, and t-3, whereas in controls, RSFC activity in the superior temporal gyrus (STG) does not depend on prior activity from any ROI.

(b) In the pediatric BD group, spontaneous activity in the amygdala depends on that of the accumbens at t-1 and t-2, whereas in controls, this relationship was mutual, with amygdala spontaneous activity depending on accumbens activity at t-1, t-2 and t-4 and accumbens activity depending on amygdala activity at t-1, t-2.

(c) In the pediatric BD group, spontaneous activity in the accumbens and the DLPFC mutually influenced one another, whereas in controls, spontaneous activity in the accumbens and DLPFC were not dependent on one another.

We used MAR modeling to formally test for between-group differences in connectivity coefficients with Bonferroni correction applied for multiple comparisons (4 lags x 16 coefficients per lag = 64 tests). We found significant between-group differences in the DLPFC's influence on the STG at time t-1 and t-2: a larger effect for BD group at t-1, and a smaller effect of BD at t-2. Additionally, the connectivity coefficient for the accumbens' influence on the DLPPC at time t-2

was smaller in the BD than the HC group. The connectivity coefficient for the amygdala's influence on the accumbens at t-2 was larger for the BD than the HC group.

MAR Discussion. Beyond DLPFC-STG findings, MAR analyses detected differences in striatal connectivity. Controls had a bi-directional relationship between the accumbens and amygdala, two highly-connected regions mediating processing of rewarding and emotionally-valenced stimuli (5;6). Yet, this relationship was unilateral in BD participants. Furthermore, BD participants had a bi-directional relationship between the accumbens and DLPFC, a relationship not detected in controls. Importantly, with respect to MAR modeling, we note the important distinction between physiological causality and Granger-causality, with the latter being a mathematical model used to explore sequential relationship between BOLD signal peaks whose inference at the neuronal level remains unknown (4;7). Behavioral deficits on tasks involving reward and face processing have been repeatedly found in pediatric BD (8-13), along with amygdala and striatal dysfunction in fMRI studies (14-17). Our current task-independent RSFC data suggest that pediatric BD may involve a fundamental alteration in fronto-temporal connectivity that potentially underlies these brain/behavior alterations.

Post-Hoc Voxel-based Morphometry (VBM) Analysis

VBM Methods. To determine if we could replicate our original VBM volumetric findings (18), we used FSL's VBM Tool software (19;20). Image preprocessing included: 1) brain-extraction using FSL's Brain Extraction Tool (BET) (21), 2) tissue segmentation into gray matter, white matter, and cerebrospinal fluid maps using FSL's Automated Segmentation Tool (FAST4) (22); 3) alignment of the gray-matter partial volume images to the MNI152 standard space using the affine registration via FSL's Linear Registration Tool (FLIRT) followed by non-

linear registration using FSL's Non-linear Image Registration Tool (FNIRT) using b-spine representation of the original registration warp field (23), 4) creation of a study-specific template from the average of these resultant images, 5) non-linear registration of native gray matter images, 6) modulation of registered partial volume images to correct for local tissue expansion/contraction by dividing by the Jacobian of the warp field, and 7) smoothing of modulated segmented images with a 3 mm isotropic Gaussian kernel. Voxel-wise general linear model was applied for between-group comparisons examined at p = 0.05 uncorrected in the a priori ROIs of the left DLPFC, left amygdala, and left accumbens area.

VBM Results. To determine if we could replicate our original VBM volumetric findings, we used FSL's VBM Tool software. We found that BD participants had decreased volume in our a priori region of the left DLPFC, although not surprisingly given our smaller sample size, this was at a lower statistical threshold ($p_{\text{uncorrected}} = 0.05$) and slightly posterior to our original finding (x = -44, y = 24, z = 38) (Figure S2).

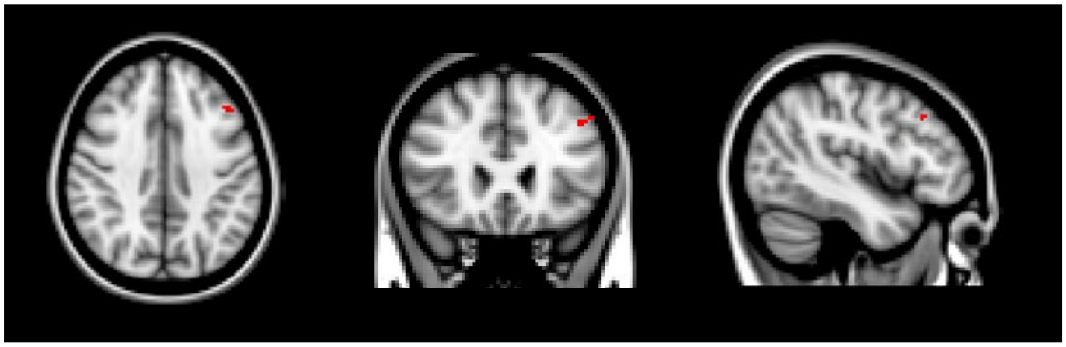

Figure S2. Decreased left dorsolateral prefrontal cortex (DLPFC) volume in pediatric bipolar disorder (N = 15) vs. control (N = 15) participants. Note: Red indicates decreased left DLPFC volume $p_{\text{uncorrected}} = 0.05$ in a priori region of interest. Method: 3 Tesla Siemens Tim Trio MPRAGE Scan ($TR_{\text{epetition}} = 2250$ ms, $TE_{\text{cho}} = 2.98$ ms, T1 = 900 ms, flip angle = 90^0, slices = 160, field of view = 256 mm, voxels = 1 x 1 x 1 mm, duration = 7.36 min) analyzed with FSL's VBM Tool.

Post-hoc Analyses: Development, Medication, Global Signal Correction (GSC), and ROI Selection

We examined the potential role of development by conducting post-hoc correlations between extracted RSFC data from our primary analyses above vs. age and Tanner pubertal stage. The main finding was that age was significantly correlated with RSFC between the right STG and right parahippocampal gyrus for both groups, although in opposite directions (BD Pearson = 0.51, $p = 0.05$; HC Pearson = -0.58, $p = 0.02$). Controls also had significant correlation between this region and Tanner stage by pubic hair (Pearson = -0.51, $p = 0.05$) but not breast/testes growth (Pearson = -0.45, $p = 0.10$). BD participants had no significant correlations with Tanner stage, but did have significant correlations between age and the left middle frontal gyrus (Pearson = -0.56, $p = 0.03$), right superior frontal gyrus (Pearson = -0.60, $p = 0.02$), and left thalamus/caudate body (Pearson = -0.74, $p = 0.001$). Thus, developmental effects on RSFC in pediatric BD bear further study.

To evaluate potential medication effects, we conducted post-hoc t-tests using extracted RSFC data from our primary analyses and did not find any significant differences between BD participants taking (a) lithium vs. not (9 vs. 6), (b) atypical neuroleptics vs. not (13 vs. 2), or (c) usually on stimulants vs. not (6 vs. 9). We then compared (a) BD participants not on lithium vs. all controls (6 vs. 15) and (b) BD participants not usually on ADHD stimulants vs. all controls (9 v. 15). Both comparisons confirmed our primary findings—i.e., BD participants not taking either lithium or stimulants had altered RSFC between the DLPFC and the STG, and iteratively, between the STG and left middle frontal, right superior frontal, left thalamus/caudate, and right parahippocampal gyri.

To avoid potential type II error in lack of amygdala findings in our primary analyses, we re-analyzed our data using amygdala and accumbens ROIs from the Harvard-Oxford Brain Atlas. There were no significant differences with the left amygdala, left accumbens, or right accumbens anatomical ROIs, but we did find significantly decreased RSFC in BD vs. HC participants between the right amygdala and the left STG (BA22) (cluster size 1056, $p_{\text{corrected}} = 0.006$, Z = 4.47, x = -56, y = 12, z = -2). Thus, we confirmed that our failure to find altered RSFC between the left amygdala and left accumbens was not due to using spherical seeds based on Dickstein *et al.* 2005 (18) rather than anatomic ROIs.

To evaluate the impact of GSC on our primary results, we re-preprocessed and re-analyzed our data without GSC. There were no significant whole-brain corrected between-group differences between the left DLPFC and any region, or between the right STG and any region. However, extracted data from the regions from our primary analyses—now processed without GSC—(a) shows the same overall pattern but with greater variance (standard deviations) and (b) is significantly different, though as expected, at a lower level than that with GSC (Figure S3, Table S1). In short, this suggests that GSC successfully reduces inter-subject variability without disproportionately affecting one group.

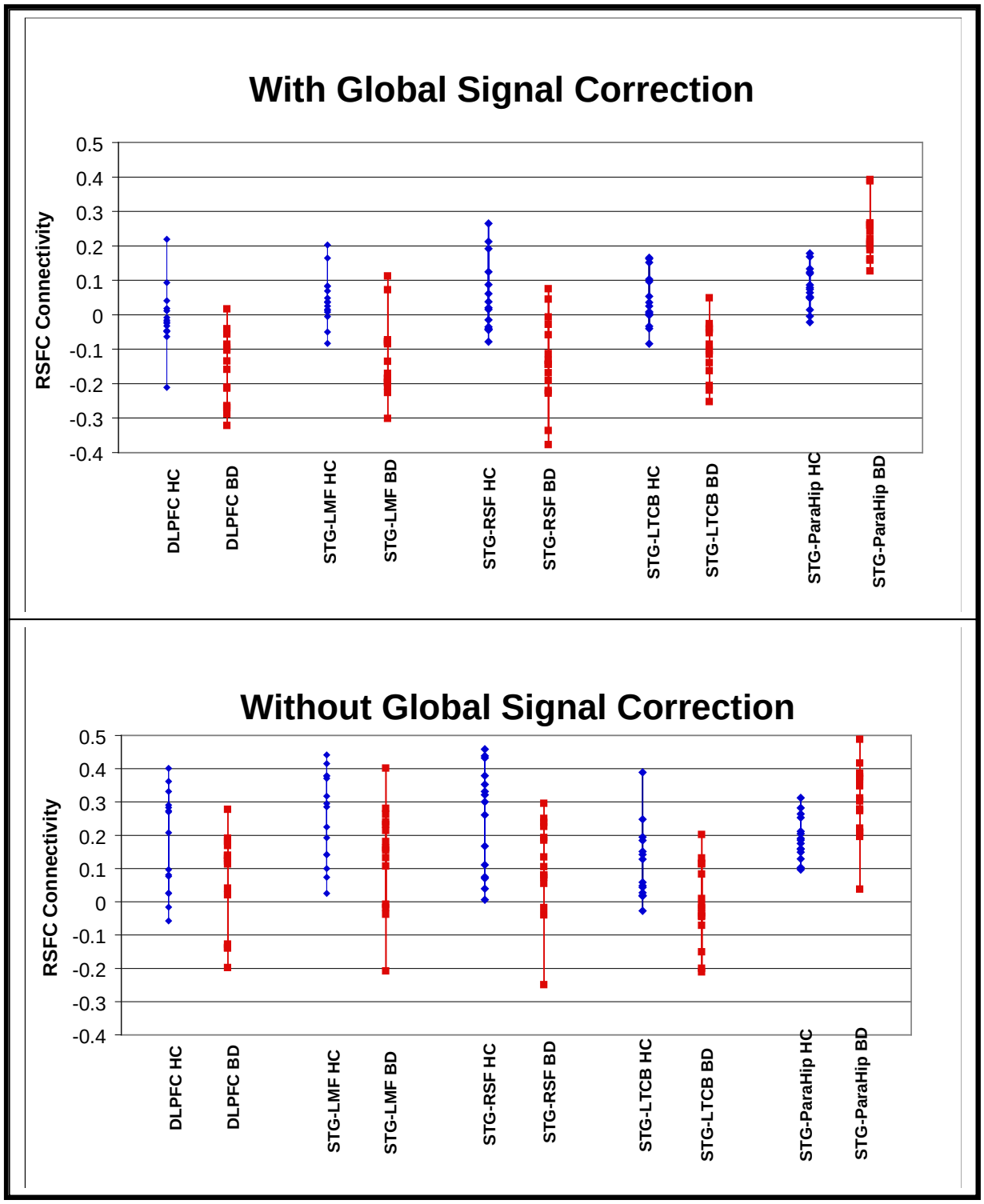

Figure S3. Comparison of extracted resting state functional connectivity (RSFC) data from primary analyses processed with global signal correction (GSC) [top] and without GSC [bottom]. BD, bipolar disorder; DLPFC, dorsolateral prefrontal cortex; HC, healthy controls; LMF, left middle frontal; LTCB, left thalamus/caudate body; ParaHip, parahippocampal gyrus; RSF, right superior frontal; STG, superior temporal gyrus.

Table S1. Comparison of processing with global signal correction (GSC; left) and without GSC (right)

		Processed with Global Signal Correction					**Processed *WITHOUT* Global Signal Correction**				
Seed	**Region**	**Group**	**Mean+SD**	**df**	**t**	**p**	**Group**	**Mean+SD**	**df**	**t**	**p**
Left DLPFC	Right STG	BD	-0.167±0.104	28	4.42	0.000	BD	0.061±0.146	28	2.14	0.04
		HC	-0.009±0.091				HC	0.177±0.150			
Iterative Right STG	Left Middle Frontal Gyrus (BA9)	BD	-0.129±0.111	28	5.04	0.000	BD	0.140±0.154	28	2.14	0.04
		HC	0.043±0.073				HC	0.252±0.134			
	Right Superior Frontal Gyrus (BA9)	BD	-0.136± 0.128	28	4.35	0.000	BD	0.107±0.139	28	2.63	0.01
		HC	0.051±0.105				HC	0.250±0.157			
	Left Thalamus and Caudate Body	BD	-0.103±0.082	28	5.03	0.000	BD	-0.009±0.122	28	2.78	0.01
		HC	0.043±0.077				HC	0.110±0.112			
	Right Para-Hippocampal Gyrus	BD	0.236±0.075	28	-6.42	0.000	BD	0.294±0.111	28	-3.11	0.004
		HC	0.078±0.589				HC	0.192±0.064			

DLPFC, dorsolateral prefrontal cortex; STG, superior temporal gyrus, BD, bipolar disorder; HC, healthy controls

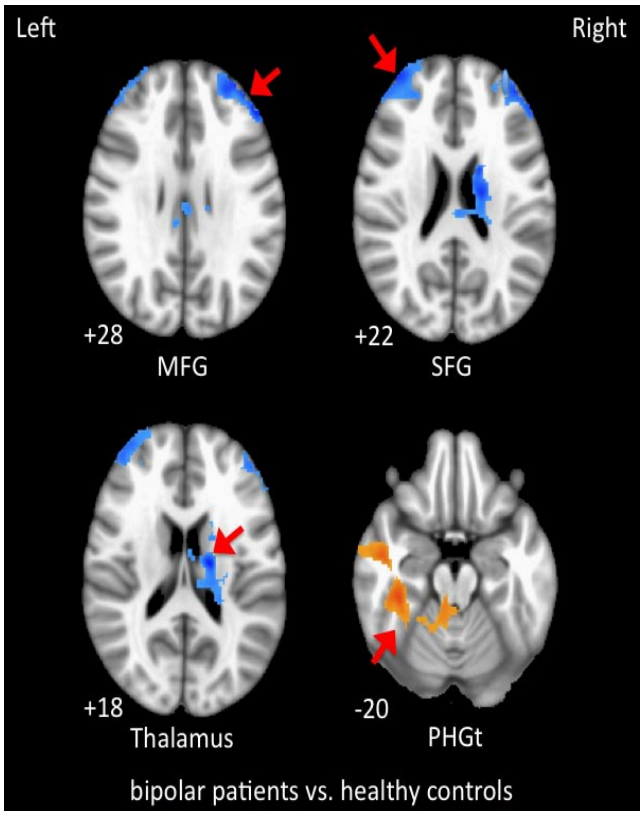

Figure S4. Additional images of significantly altered resting state functional connectivity (RSFC) between right superior temporal gyrus (STG) and fronto-temporal regions in pediatric bipolar disorder (BD, N = 15) vs. typically-developing healthy dontrols (HC, N = 15). Note: This figure supplements Figure 1B. Significantly decreased (blue) RSFC activity in BD vs. control youths between the right STG and: 1) left middle frontal gyrus (MFG, BA9, x = -48, y = 36, z = 28; Voxels = 953, $p_{corrected} = 0.009$), 2) right superior frontal gyrus (SFG, BA9, x = 38, y = 58, z = 22; Voxels = 809, $p_{corrected} = 0.02$), and 3) left thalamus/caudate body (x = -16, y = -12, z = 18; Voxels = 688, $p_{corrected} = 0.05$). Significantly increased (orange) RSFC between STG and right parahippocampal gyrus (PHG, BA36, x = 38, y = -32, z = -20; Voxels = 1931, $p_{corrected} = 0.00007$). Method: 3 Tesla Siemens Tim Trio BOLD scan ($TR_{repetition} = 2000$ msec, $TE_{cho} = 25$ ms, flip angle = 90^0, slices = 35, field of view = 192 mm, voxels = 3 x 3 x 3 mm, duration = 8.36 minutes) acquired while participant was at rest.

1. Goebel R, Roebroeck A, Kim DS, Formisano E (2003): Investigating directed cortical interactions in time-resolved fMRI data using vector autoregressive modeling and Granger causality mapping. *Magn Reson Imaging* 21:1251-1261.
2. Harrison L, Penny WD, Friston K (2003): Multivariate autoregressive modeling of fMRI time series. *Neuroimage* 19:1477-1491.
3. Shumway RH, Stoffer DS (2006): *Time Series Analysis and Its Applications: With R Examples*, Second ed. New York, NY: Springer.
4. Cole DM, Smith SM, Beckmann CF (2010): Advances and pitfalls in the analysis and interpretation of resting-state FMRI data. *Front Syst Neurosci* 4:8.
5. Schoenbaum G, Setlow B (2003): Lesions of nucleus accumbens disrupt learning about aversive outcomes. *J Neurosci* 23:9833-9841.
6. Bray S, O'Doherty J (2007): Neural coding of reward-prediction error signals during classical conditioning with attractive faces. *J Neurophysiol* 97:3036-3045.
7. Roosendaal SD, Schoonheim MM, Hulst HE, Sanz-Arigita EJ, Smith SM, Geurts JJ, *et al.* (2010): Resting state networks change in clinically isolated syndrome. *Brain* 133:1612-1621.
8. McClure EB, Pope K, Hoberman AJ, Pine DS, Leibenluft E (2003): Facial expression recognition in adolescents with mood and anxiety disorders. *Am J Psychiatry* 160:1172-1174.
9. Dickstein DP, Treland JE, Snow J, McClure EB, Mehta MS, Towbin KE, *et al.* (2004): Neuropsychological performance in pediatric bipolar disorder. *Biol Psychiatry* 55:32-39.
10. Ernst M, Dickstein DP, Munson S, Eshel N, Pradella AG, Jazbec S, *et al.* (2004): Reward-related processes in pediatric bipolar disorder: a pilot study. *J Affect Disord* 82:S89-S101.
11. Gorrindo T, Blair RJ, Budhani S, Dickstein DP, Pine DS, Leibenluft E (2005): Deficits on a probabilistic response-reversal task in patients with pediatric bipolar disorder. *Am J Psychiatry* 162:1975-1977.
12. Dickstein DP, Nelson EE, McClure EB, Grimley ME, Knopf L, Brotman MA, *et al.* (2007): Cognitive flexibility in phenotypes of pediatric bipolar disorder. *J Am Acad Child Adolesc Psychiatry* 46:341-355.

13. Brotman MA, Guyer AE, Lawson ES, Horsey SE, Rich BA, Dickstein DP, *et al.* (2008): Facial emotion labeling deficits in children and adolescents at risk for bipolar disorder. *Am J Psychiatry* 165:385-389.
14. Rich BA, Vinton DT, Roberson-Nay R, Hommer RE, Berghorst LH, McClure EB, *et al.* (2006): Limbic hyperactivation during processing of neutral facial expressions in children with bipolar disorder. *Proc Natl Acad Sci U S A* 103:8900-8905.
15. Leibenluft E, Rich BA, Vinton DT, Nelson EE, Fromm SJ, Berghorst LH, *et al.* (2007): Neural circuitry engaged during unsuccessful motor inhibition in pediatric bipolar disorder. *Am J Psychiatry* 164:52-60.
16. Nelson EE, Vinton DT, Berghorst L, Towbin KE, Hommer RE, Dickstein DP, *et al.* (2007): Brain systems underlying response flexibility in healthy and bipolar adolescents: an event-related fMRI study. *Bipolar Disord* 9:810-819.
17. Pavuluri MN, O'Connor MM, Harral EM, Sweeney JA (2008): An fMRI study of the interface between affective and cognitive neural circuitry in pediatric bipolar disorder. *Psychiatry Res* 162:244-255.
18. Dickstein DP, Milham MP, Nugent AC, Drevets WC, Charney DS, Pine DS, *et al.* (2005): Frontotemporal alterations in pediatric bipolar disorder: results of a voxel-based morphometry study. *Arch Gen Psychiatry* 62:734-741.
19. Ashburner J, Friston KJ (2000): Voxel-based morphometry--the methods. *Neuroimage* 11:805-821.
20. Good CD, Johnsrude IS, Ashburner J, Henson RN, Friston KJ, Frackowiak RS (2001): A voxel-based morphometric study of ageing in 465 normal adult human brains. *Neuroimage* 14:21-36.
21. Smith SM (2002): Fast robust automated brain extraction. *Hum Brain Mapp* 17:143-155.
22. Zhang Y, Brady M, Smith S (2001): Segmentation of brain MR images through a hidden Markov random field model and the expectation-maximization algorithm. *IEEE Trans Med Imaging* 20:45-57.
23. Jenkinson M, Smith S (2001): A global optimisation method for robust affine registration of brain images. *Med Image Anal* 5:143-156.